Journal of Electrocardiology 51 (2018) 239–246

Contents lists available at ScienceDirect

Journal of Electrocardiology

journal homepage: www.jecgonline.com

Automatic activation mapping and origin identification of idiopathic outflow tract ventricular arrhythmias

Alejandro Alcaine, PhD [a,b], David Soto-Iglesias, PhD [c,d], Juan Acosta, MD [d], Viatcheslav Korshunov, MD [c,d], Diego Penela, MD, PhD [d], Mikel Martínez, MD [c,d], Markus Linhart, MD [c,d], David Andreu, PhD [d], Juan Fernández-Armenta, MD, PhD [d], Pablo Laguna, PhD [a,b], Juan Pablo Martínez, PhD [a,b], Oscar Camara, PhD [e], Antonio Berruezo, MD, PhD [c,d,*]

[a] BSICoS Group, Aragón Institute of Engineering Research (I3A), IIS Aragón, Universidad de Zaragoza, Zaragoza, Spain
[b] CIBER en Bioingeniería, Biomateriales y Nanomedicina (CIBER-BBN), Madrid, Spain
[c] Arrhythmia Section, Cardiology Dept., Thorax Institute, Hospital Clínic, Universitat de Barcelona, Barcelona, Spain
[d] IDIBAPS (Institut d'Investigació Agustí Pi i Sunyer), Barcelona, Spain
[e] Physense Group, Dept. of Information and Communication Technologies, Universitat Pompeu Fabra, Barcelona, Spain

ARTICLE INFO

Keywords:
Activation mapping
Idiopathic ventricular arrhythmia
Left ventricle outflow tract
Right ventricle outflow tract
Ventricular tachycardia ablation

ABSTRACT

Purpose: Activation mapping is used to guide ablation of idiopathic outflow tract ventricular arrhythmias (OTVAs). Isochronal activation maps help to predict the site of origin (SOO): left *vs* right outflow tract (OT). We evaluate an algorithm for automatic activation mapping based on the onset of the bipolar electrogram (EGM) signal for predicting the SOO and the effective ablation site in OTVAs.
Methods: Eighteen patients undergoing ablation due to idiopathic OTVAs were studied (12 with left ventricle OT origin). Right ventricle activation maps were obtained offline with an automatic algorithm and compared with manual annotation maps obtained during the intervention. Local activation time (LAT) accuracy was assessed, as well as the performance of the 10 ms earliest activation site (EAS) isochronal area in predicting the SOO.
Results: High correlation was observed between manual and automatic LATs (Spearman's: 0.86 and Lin's: 0.85, both $p < 0.01$). The EAS isochronal area were closely located in both map modalities (5.55 ± 3.56 mm) and at a similar distance from the effective ablation site (0.15 ± 2.08 mm difference, $p = 0.859$). The 10 ms isochronal area longitudinal/perpendicular diameter ratio measured from automatic maps showed slightly superior SOO identification (67% sensitivity, 100% specificity) compared with manual maps (67% sensitivity, 83% specificity).
Conclusions: Automatic activation mapping based on the bipolar EGM onset allows fast, accurate and observer-independent identification of the SOO and characterization of the spreading of the activation wavefront in OTVAs.

Introduction

Catheter ablation is becoming the therapy of choice for antiarrhythmic drug-resistant ventricular arrhythmias (VAs), whether or not structural heart disease is present [1]. Idiopathic VAs are defined as those occurring in patients without structural heart disease [1], and frequently originate in outflow tract regions [2–4]. Activation mapping using an electroanatomical mapping system helps to determine the earliest activation site (EAS), the target for radiofrequency (RF) ablation in idiopathic outflow tract ventricular arrhythmias (OTVAs) [5,6].

The OTs have complex 3-dimensional anatomical relationships [5,7,8], which makes the identification of the site of origin (SOO) especially challenging when maximal electrogram (EGM) precocity occurs in the septal right ventricle outflow tract (RVOT), where the SOO can be located either in the RVOT or in the left ventricle outflow tract (LVOT). In those cases, the analysis of isochronal activation maps improves SOO prediction, compared to surface electrocardiogram (ECG) algorithms [4,9]. On the other hand, there is no established consensus about what is the appropriate signal feature to assess local activation time (LAT) from bipolar EGMs for activation mapping [10,11]. Furthermore, acquisition of detailed activation maps using the bipolar EGM signal onset turns into a manual, time-consuming, operator-dependent task performed under stressful conditions within the electrophysiology lab.

Recently, a novel algorithm for automatic activation mapping based on LATs identified from the bipolar EGM signal onset was introduced [12] and improved by inclusion of spatial information from close mapping points, yielding reliable and spatially consistent automatic activation maps [13]. Therefore, this algorithm provides an operator-independent

* Corresponding author at: Arrhythmia Section, Cardiology Department, Thorax Institute, Hospital Clínic, C/ Villarroel 170, 08036 Barcelona, Spain.
E-mail address: berruezo@clinic.cat

https://doi.org/10.1016/j.jelectrocard.2017.10.015
0022-0736/

estimation of LATs based on the bipolar EGM signal onset for automatic activation mapping and activation pattern assessment.

The inclusion in electroanatomical mapping (EAM) systems of a reliable automatic algorithm that systematically identifies LATs on a reproducible manner will help to assess activation patterns and to identify at a glance the origin of the arrhythmia, thus may contribute in improving ablation treatment and procedure times. In the present study, we aimed to validate two aspects of the automatic activation mapping methodology, first comparing its LAT precision with manual LAT annotations obtained during the intervention and second assessing its ability to precisely identify the EAS area and predict the SOO (RVOT *vs* LVOT) in patients with idiopathic OTVAs. For this latter purpose, map descriptors based on the size and shape of the 10 ms EAS isochronal area on manual and automatic right ventricle (RV) activation maps were measured and evaluated.

Materials and methods

Patient Sample

A group of 18 patients (12 of them with V3 transition) with symptomatic, drug-refractory, outflow tract premature ventricular contraction (PVC) beats and admitted for RF ablation at a single centre were included in the study. All patients signed their written informed consent to participate in the study. Inclusion criteria were as follows: (1) patients with idiopathic OTVAs admitted for ablation; (2) EAS located at the septal part of the RVOT electroanatomical map and (3) successful ablation at the EAS identified by manual activation mapping during the intervention. All measurements were obtained offline from manual and automatic activation maps; therefore, ablation outcomes did not depend on the data obtained for this study. The local Ethics Committee approved the study.

Mapping and ablation procedure

Patient electroanatomical maps were acquired with the CARTO 3 system (Biosense Webster, Inc., Diamond Bar, CA, USA) using a 3.5 mm irrigated tip NaviStar Thermocool catheter (Biosense Webster, Inc., Diamond Bar, CA, USA) for mapping and ablation. The 12-lead surface ECG and EGM signals were acquired at 1 kHz sampling frequency, displayed during each intervention and stored for offline prospective analysis. EGM signals were acquired point-by-point during stable contact with the myocardium, pulmonary and aortic root walls; during mapping, operators ensured the presence of PVCs that matched the clinical VA.

During the intervention, the EAM system operator carefully annotated the onset of the distal electrode bipolar EGM signal from the mapping catheter as the start of the first steepest deflection. Detailed activation mapping of the RVOT was performed during PVCs. Accordingly to a previous study [9], a LVOT origin was suspected when the EAS of the RVOT isochronal activation map was located ≥1 cm below the pulmonary valve or the 10 ms isochronal area longitudinal/perpendicular diameter ratio was ≤0.8. If LVOT origin was suspected, the distal coronary sinus (CS), great cardiac vein, left anterior descendent vein, supra- and subvalvular LVOT were mapped as part of the electrophysiological study protocol. After the acquisition of a sufficient number of mapping points to reconstruct the anatomy and activation pattern, using a filling threshold of 6 mm, RF was delivered at the EAS with a power limit of 40 W in the RVOT, subvalvular LVOT and aortic root, and 20 W in the CS.

Automatic EGM delineation algorithm

The automatic RV activation map was obtained offline using an algorithm to delineate the activation onset of bipolar EGM signals implemented in Matlab (Matlab R2010a, The Mathworks, Inc., Natick, MA, USA). Briefly, the algorithm uses the 12-lead surface ECG as a reference window to identify the EGM of interest and delineates its onset and end time landmarks using the wavelet transform of the envelope of the bipolar EGM signal [12]. Then, LAT estimation is obtained by measuring the time difference between the bipolar EGM onset landmark to the reference ECG lead (as shown in Fig. 1). Additionally, a "spatial" signal-averaging algorithm, considering close mapping points with a morphologically similar EGM signal, was used to improve activation maps [13]. This method provides more reliable measurements, especially in the high-density mapping areas that are usually an area of interest for ablation of focal VAs [13]. Fig. 1 shows representative examples of bipolar EGMs and the onset and end time landmarks automatically identified by the algorithm and the manually identified onset landmarks.

Map Reconstruction

LATs identified by the automatic delineation algorithm were manually entered in the CARTO system for evaluation. Manual and automatic 3-D RV electroanatomical activation maps were reconstructed using an interpolation filling threshold of 6 mm. Isochronal activation areas were obtained by discrete division of the color scale, starting from the earliest activated point and color-coded from red (earliest activated) to purple (latest activated) in 10 ms steps.

Map descriptors

The map descriptors used in this study characterize the extent and spreading of the activation pattern in RV activation maps during PVCs. The size of the 10 ms EAS isochronal area and its longitudinal and perpendicular diameters relative to the RVOT axis were measured as described by Herczku et al. [4]. The longitudinal diameter was defined by the line parallel to the septal projection of the RVOT longitudinal axis (perpendicular to the plane of the pulmonary valve) and then the perpendicular diameter was obtained. The spreading of the activation pattern was characterized by defining the ratio between those two axes, which has been used to discriminate between RVOT and LVOT origin of idiopathic OTVAs [4,9].

In the RVOT SOO population activation maps, the accuracy of the automatic algorithm in locating the 10 ms EAS isochronal area for effective ablation was quantified by measuring two distances: (1) from the centre of mass of the 10 ms EAS isochronal area to the effective ablation point and (2) between the centres of mass of the 10 ms EAS isochronal areas indicated on manual and automatic maps. Left ventricle activation maps (from LVOT SOO population cases) were not considered for this specific measurement because they did not meet the filling threshold criterion (6 mm), thus had lower density of mapping points compared with RV activation maps.

Isochronal areas were obtained at 10 ms steps as described before, and the measurements were done using the CARTO 3 integrated measurement tools. Hence, the difference between measures is related only to the method for LAT detection, i.e., manual versus automatic LATs.

Statistical analysis

Continuous data are shown in mean ± standard deviation unless otherwise indicated and categorical data are shown as percentages. Populations were compared by the Wilcoxon-Mann-Whitney or Fisher exact test, as appropriate. Correlation between automatic and manual LATs was determined using the Spearman rank correlation coefficient and checked with Lin's concordance correlation coefficient [14]. Bland-Altman plots were used to assess agreement between automatic and manual LATs. A p-value ≤ 0.05 was considered as cut-off value for statistical significance. Statistics were obtained using the Matlab's statistics toolbox (Matlab R2010a, The Mathworks, Inc., Natick, MA, USA) and custom software when needed.

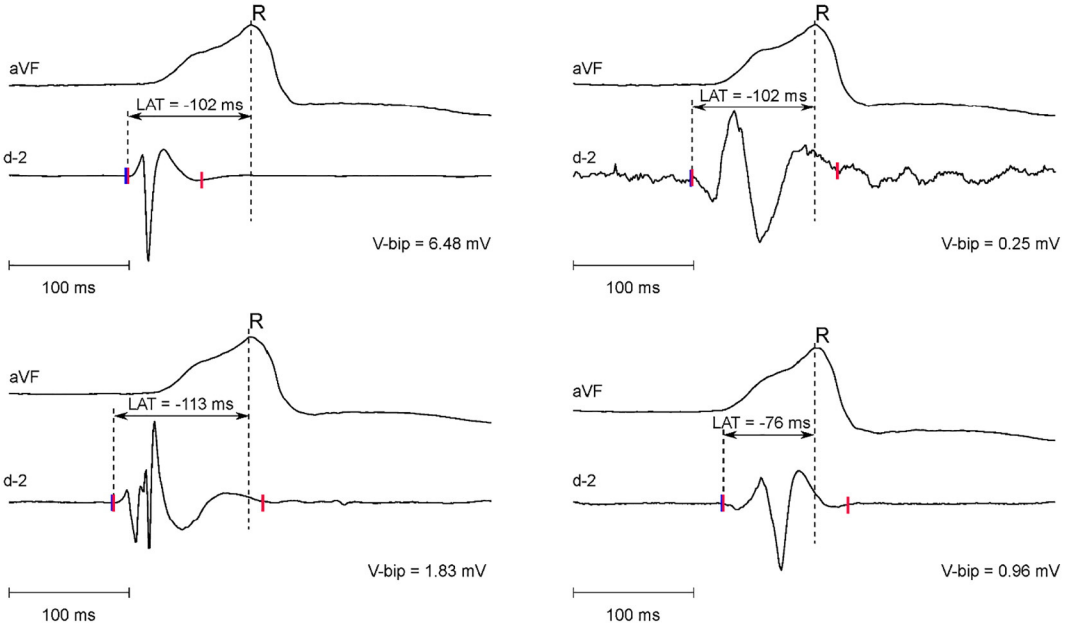

Fig. 1. Example of electrogram (EGM) signals from different mapping points (top line: reference aVF surface ECG lead, bottom line: bipolar distal (d-2) EGM signal), the manually identified onset landmark with vertical blue line and the automatically detected onset and end landmarks were indicated with vertical red lines. Vertical dashed line marked with an R indicates the reference time for computation of local activation time (LAT). V-bip stands for the peak-to-peak bipolar EGM voltage.

Results

Population characteristics

Eighteen patients were included in the study (50% men, mean age 56.3 ± 16.6 years, 33.3% hypertensive). Table 1 summarizes the baseline characteristics of the study population. The mean PVC burden during an ambulatory 24-h-Holter recording performed before the procedure was 27.9 ± 10.9%. Ablation was successful (i.e., elimination of 100% extrasystole events during the procedure) in all 18 patients, 12 of them in the LVOT (9 in left/right coronary cusp and 3 in subvalvular LVOT) and 6 in the septal RVOT. The median [interquartile range] number of RF applications was 3 [1–8] and mean RF time was 6 ± 6.7 min. No complications were observed.

Activation identification accuracy

The automatically identified LATs were compared against the manual LATs, both based on the bipolar EGM signal onset landmark. Mean and standard deviation of the differences between all LAT annotations was 7.13 ± 12.29 ms (see Supplementary Table 1). Spearman's rank correlation was 0.86 ($p < 0.01$) and Lin's concordance correlation was 0.85 ($p < 0.01$). Bland-Altman plot analysis (Fig. 2.a, bottom panel) showed a small trend (Pearson's correlation: 0.21, $p < 0.01$) towards an underestimation of LAT precocity by the automatic algorithm, compared with the manual method.

Differences between automatic and manual LAT estimates were greater in the LVOT population, compared to the RVOT population (8.77 ± 12.70 ms *vs* 3.73 ± 10.61 ms, $p < 0.01$), and produced lower Spearman's rank correlation (0.86 *vs* 0.90) and Lin's concordance correlation (0.82 *vs* 0.91) coefficients. Bland-Altman analysis of both LVOT and RVOT populations (bottom panels of Fig. 2.b and c, respectively) indicated almost the same low Pearson's correlation (0.22 and 0.23, respectively, both $p < 0.01$). Representative examples of 3-D reconstruction of activation maps using manual or automatically identified LATs are shown in Fig. 3.

Earliest activation site identification

The distance from the centroid of the 10 ms EAS isochronal area to the effective RF application point was similar in both the automatic and manual activation maps in the RVOT population (0.15 ± 2.08 mm

Table 1
Baseline characteristics of the patient sample.

	Entire population ($n = 18$)	RVOT SOO ($n = 6$)	LVOT SOO ($n = 12$)	p-Value[a]
Age, years	56.3 ± 16.6 58 [45–72]	51.5 ± 15.8 45 [39–69]	58.8 ± 17.1 60 [53–72]	0.372
Male sex, n (%)	9 (50)	2 (33.3)	7 (58.3)	0.244
Hypertension, n (%)	6 (33.3)	1 (16.7)	5 (41.6)	0.256
Mapping characteristics				
Mapping points, n	175 ± 61 169 [120–240]	172 ± 47 155 [148–181]	177 ± 69 183 [112–247]	1.000
Total RF applications, n	6 ± 6 3 [1–8]	2 ± 2 2 [1–3]	7 ± 7 4 [1–12]	0.259
RF applications on RVOT, n	3 ± 4 2 [0–4]	2 ± 2 2 [1–3]	3 ± 4 1 [0–5]	0.556

Values are given as mean ± standard deviation and median [1st quartile-3rd quartile] or n (%).
LVOT – left ventricle outflow tract, RF – radio frequency, RVOT – right ventricle outflow tract, SOO – site of origin.
[a] Comparison between measures at RVOT and LVOT SOO.

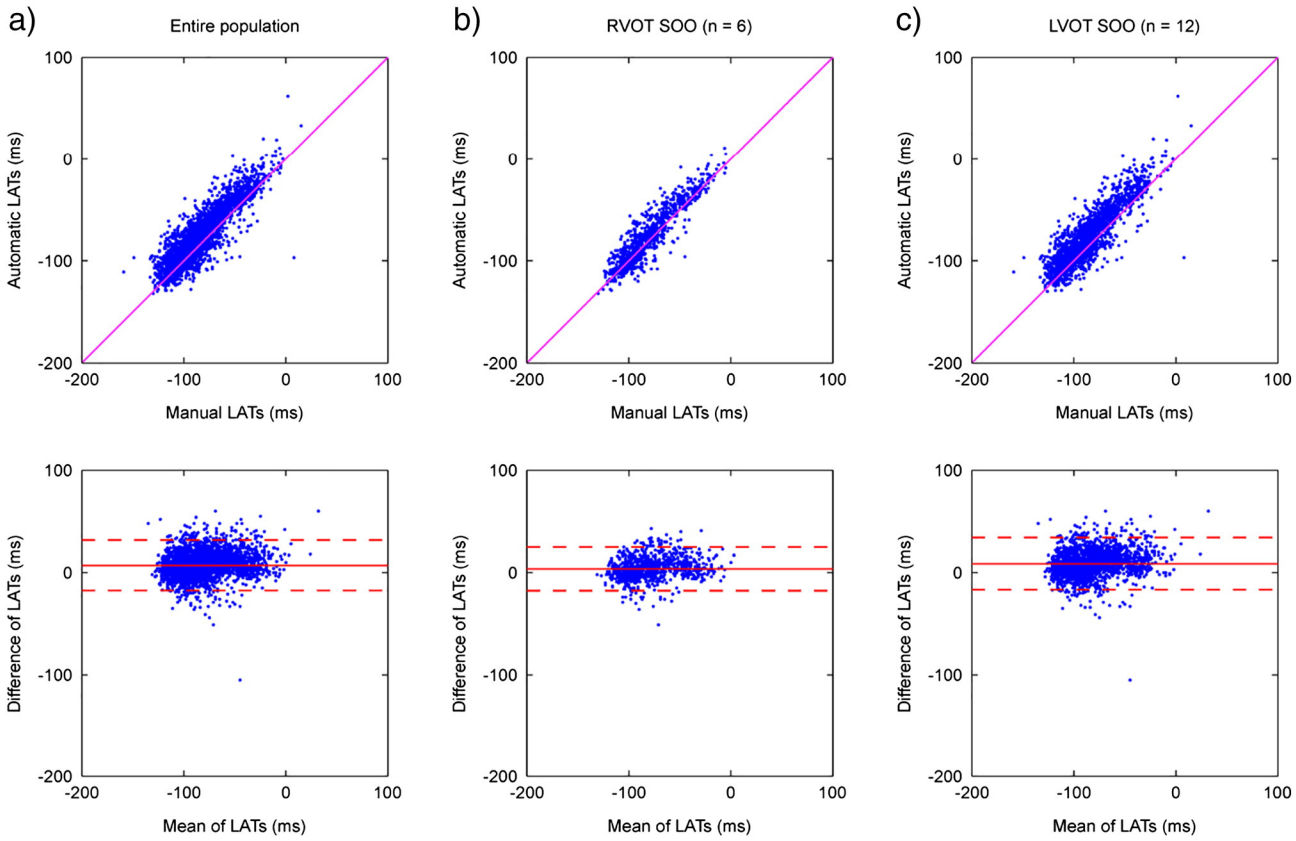

Fig. 2. Scatterplots (top panels) and Bland-Altman plot (bottom panels) of the comparison between automatic and manual local activation times (LATs) in three populations: a) the whole sample, b) right ventricle outflow tract (RVOT) site of origin (SOO) and c) left ventricle outflow tract (LVOT) SOO. Pink continuous line indicates the identity line. Red continuous line indicates mean LAT difference and red dashed lines indicate mean ± 2 times standard deviation of LAT difference.

difference, $p = 0.859$). A short distance was observed between the centroids identified from manual and automatic maps (5.55 ± 3.56 mm), as shown in Table 2.

Assessment of map descriptors measurement and SOO identification

In the LVOT population, significant differences were observed in the size of the 10 ms EAS isochronal area determined from the automatic *vs* manual activation maps (Table 3). Automatic maps showed smaller 10 ms EAS isochronal areas compared with the manual maps (2.11 ± 1.59 cm^2 *vs* 4.37 ± 3.22 cm^2, respectively, $p = 0.040$). The rest of the map descriptor measurements showed no significant differences between automatic and manual activation maps.

On the other hand, the 10 ms isochronal area longitudinal/perpendicular diameter ratio differs significantly between RVOT and LVOT populations, whether measured from the manual activation maps (1.97 ± 0.88 *vs* 1.08 ± 0.67, $p = 0.019$) or from the automatic activation maps (2.01 ± 0.44 *vs* 0.90 ± 0.48, $p = 0.001$).

Fig. 4 and Table 4 illustrate the SOO identification. The size of the 10 ms EAS isochronal area better distinguishes between RVOT and LVOT populations if measured from manual activation maps, with 83% sensitivity and 67% specificity using an optimal threshold for LVOT SOO identification using the 10 ms EAS area ≥ 2.2 cm^2 (Fig. 4a, left panels). However, superior performance on SOO identification was achieved by the 10 ms isochronal area longitudinal/perpendicular diameter ratio, whether measured from manual or automatic activation maps. More specifically, the best SOO identification was obtained from the automatic activation map, with 92% sensitivity and 100% specificity using an optimal threshold for LVOT SOO identification using the longitudinal/perpendicular diameter ratio ≤ 1.27, yielding a SOO identification accuracy of 94% in the current patient sample (Table 4).

A previously published study showed that VAs arising from the septal RVOT should have a 10 ms EAS isochronal area whose main direction extends along the fibre orientation (i.e., activation has an elliptical shape in the longitudinal direction), whereas those arising from the LVOT should have a slower and less preferential path in the longitudinal direction in the septal RVOT (i.e., activation has a circular shape) [4,9]. This hypothesis allows us to establish a comparison between the manual and automatic activation mapping modalities using a hypothetical threshold for LVOT SOO identification ≤1 for the 10 ms isochronal area longitudinal/perpendicular diameter ratio. This decreases the automatic maps' performance on SOO identification to 67% sensitivity, 100% specificity and 78% accuracy; which remains slightly superior to the performance obtained from manual activation maps (67% sensitivity, 83% specificity and 72% accuracy). This superiority is consistent with the higher area under the curve (AUC) observed for automatic activation maps (0.94) compared with the manual activation maps (0.84), as shown in Table 4.

Discussion

The present study shows the possibilities of the automatic activation mapping approach in clinical practice. There were three main findings about the automatic delineation algorithm: (1) it accurately identified LATs, compared with manual LATs obtained during the procedure, (2) it precisely identified the location of the 10 ms EAS isochronal area for ablation purposes and (3) it showed superior performance, compared to manual activation maps, in SOO identification of idiopathic OTVAs using the 10 ms isochronal area's longitudinal/perpendicular diameter ratio.

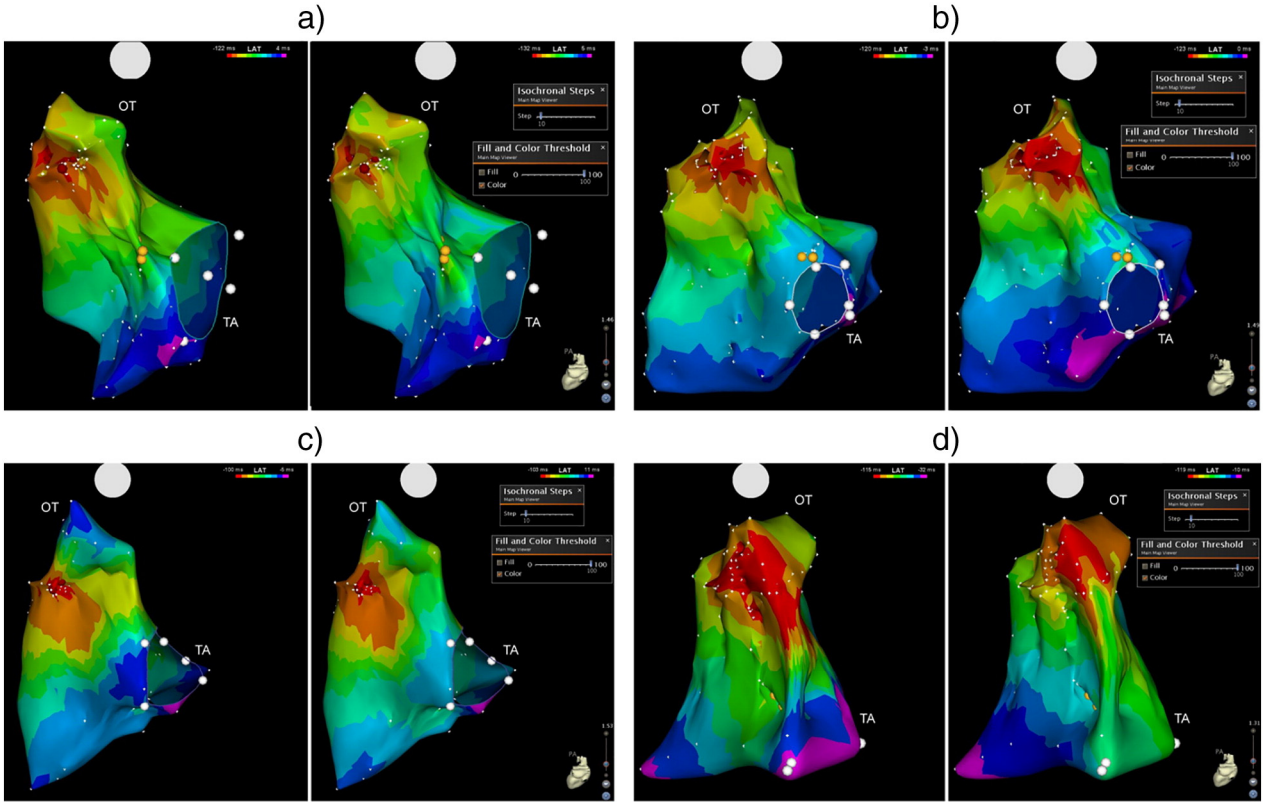

Fig. 3. Examples of right ventricle (RV) 10 ms isochronal activation maps reconstructed from the manually identified local activation times (LATs) (left picture of each panel) and from the automatically identified LATs (right picture of each panel) shown in posterior-anterior (PA) view. All maps show the early activation site (EAS) isochronal area at the septal right ventricle outflow tract (RVOT). Panels a) and c) show RV activation maps from patients with RVOT site of origin (SOO) VAs (patients #1 and #5), and panels b) and d) show RV activation maps from patients with left ventricle outflow tract SOO VAs (patients #7 and #8). White spheres indicate anatomical location, yellow spheres indicate His-Purkinje potentials and red spheres indicate radio frequency applications. OT – outflow tract, TA – tricuspid annulus.

Activation identification performance

The automatic delineation algorithm showed high correlation and small LAT difference compared with manual annotations. The LAT difference was greater and the correlation was lower for the LVOT SOO population compared with the RVOT SOO population. We hypothesize that this greater LAT differences between manual and automatic maps observed in LVOT population may be due to the complex anatomical relationships between LVOT and RVOT structures [5,7,8] and/or far-field signals measured at RVOT level coming from the LVOT. These far-field signals are usually shown as low amplitude baseline drifts in the bipolar EGM signal that are difficult to distinguish from baseline noise level using the automatic algorithm, thus yielding LAT discrepancies compared with manual annotation (illustrated in the Supplementary Fig. 1). This is in accordance with the positive-bias difference, which indicates that the automatic algorithm tends to provide later LATs than the reference method. Therefore, LAT detection in LVOT SOO with septal activation at the RVOT level presents a challenge for automatic detection.

However, as illustrated in Fig. 3, such differences in LAT estimation do not imply low quality of the activation maps and activation patterns. In addition, manual LAT identification based on the onset of the bipolar EGM signal is a time-consuming, observer-dependent task performed during stressful conditions, which may affect ablation outcomes. In a previous work [12], the automatic algorithm was compared against LAT annotations from two different experts, showing LAT differences comparable to manual annotations performed during the procedure; moreover, automatic LAT detection was performed in <1 s per mapping point, in contrast to 3–4 s that may be required to perform this task manually by a trained EAM system operator [12]. This confers an advantage to automatic detection, especially when used in combination with high-density multi-electrode catheters.

Table 2
Distance from the centre of mass of the 10 ms EAS isochronal area to the effective RF ablation site and inter-EAS isochronal area distance in the RVOT population.

Patient	Distance from the 10 ms EAS isochronal area to the RF ablation point, mm		Inter-EAS isochronal area distance, mm
	Manual maps	Automatic maps	
1	4.3	3.1	2.8
2	9.1	12.4	7.2
3	11.5	8.8	6.8
4	7.2	8.1	10
5	2.7	2.7	0
6	5.3	4.1	6.6

EAS – early activation site, RF – radio frequency, RVOT – right ventricle outflow tract.

Evaluation of ablation site identification

In the RVOT SOO population activation maps, the location of the 10 ms EAS isochronal area centroids in manual and automatic activation maps was 5.55 ± 3.56 mm apart, illustrating the accuracy of the automatic algorithm in precise localization of the EAS isochronal area. In addition, the distance from the 10 ms EAS isochronal area centroid to the effective RF application site was similar on both mapping modalities (difference: 0.15 ± 2.08 mm, $p = 0.859$). These results illustrate the accuracy of the automatic algorithm for focal VA ablation purposes.

Table 3
Map descriptors measurement.

	Entire population (n = 18)	RVOT SOO (n = 6)	LVOT SOO (n = 12)	*p*-Value[a]
Size of the 10 ms EAS isochronal area				
Manual map, cm^2	3.83 ± 3.03 2.30 [2.00–5.20]	2.77 ± 2.52 2.05 [1.50–2.30]	4.37 ± 3.22 3.85 [2.30–5.80]	0.157
Automatic map, cm^2	2.44 ± 1.99 1.95 [0.80–2.70]	3.10 ± 2.67 2.25 [0.70–5.50]	2.11 ± 1.59 1.65 [0.90–2.65]	0.767
p-Value[b]	0.117	0.971	**0.040**	
10 ms isochronal area longitudinal/perpendicular ratio				
Manual map	1.38 ± 0.85 1.06 [0.73–1.63]	1.97 ± 0.88 1.90 [1.12–2.63]	1.08 ± 0.67 0.82 [0.72–1.31]	**0.019**
Automatic map	1.27 ± 0.71 1.00 [0.74–1.83]	2.01 ± 0.44 1.99 [1.72–2.38]	0.90 ± 0.48 0.80 [0.58–1.00]	**0.001**
p-Value[b]	0.740	0.937	0,544	

Values are given in mean ± standard deviation and median [1st quartile-3rd quartile].
EAS – early activation site, LVOT – left ventricle outflow tract, RVOT – right ventricle outflow tract, SOO – site of origin.
[a] Comparison between measures at RVOT and LVOT SOO, bold if $p \leq 0.05$.
[b] Comparison between manual and automatic map measurements (rows), bold if $p \leq 0.05$.

Evaluation of map descriptors measurements

The 10 ms EAS isochronal areas in the LVOT population were significantly smaller in the measurement based on the automatic activation pattern descriptors, compared to those measured from the manual maps. This concurs with the positive-bias LAT difference described above, which supposes an under-estimation of LAT precocity and therefore a reduction in the size of the EAS isochronal area. The rest of the evaluated map descriptors showed no significant differences between the measurements from automatic or manual maps.

LVOT vs RVOT SOO identification

In previous studies it has been shown that activation pattern in septal RVOT differ depending on the SOO [4,9]. VAs arising from RVOT exhibit a longitudinal craniocaudal activation pattern, whereas in VAs with LVOT SOO the shape of the activation wavefront shows a circumferential pattern. According to these findings the longitudinal/perpendicular ratio has been proposed for the differentiation of LVOT *vs* RVOT SOO.

In the present study, the 10 ms isochronal area's longitudinal/perpendicular diameter ratio showed better performance on SOO identification, regardless of measurement from manual or automatic activation maps. The best performance was obtained from the automatic activation map using a threshold for LVOT SOO identification ≤1.27, yielding 92% sensitivity and 100% specificity, compared with 58% sensitivity and 100% specificity at a smaller threshold (≤0.91) for LVOT SOO identification using manual activation maps. For SOO identification, it is desirable to have very high specificity while preserving sensitivity, avoiding an unnecessary retrograde aortic approach for LVOT and aortic root mapping, which can increase the complication rate of OT ablation procedures.

For comparison of both mapping modalities, an evaluation of the SOO identification performance was conducted based on the rationale of the 10 ms isochronal area longitudinal/perpendicular diameter

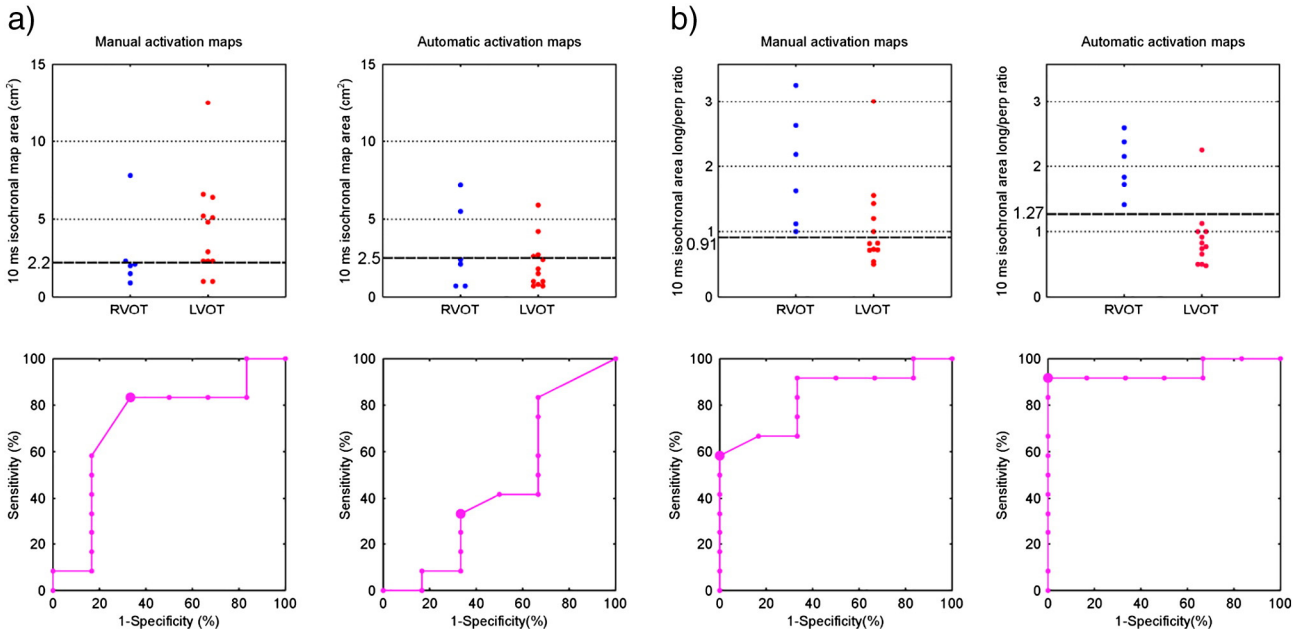

Fig. 4. Site of origin (SOO) identification by map descriptors: a) 10 ms early activation site (EAS) isochronal area and b) 10 ms isochronal area longitudinal/perpendicular diameter ratio. Top panels show scatterplots by SOO (Blue dots: left ventricle outflow tract (LVOT) SOO, red dots: right ventricle outflow tract (RVOT) SOO) measured from manual right ventricle (RV) activation maps (left panel) and from automatic RV activation maps (right panel); black dashed line indicates the optimal threshold for SOO identification. Bottom panels show the corresponding receiver operation curve; large dots indicate the optimal point for SOO identification.

Table 4
SOO identification performance of the map descriptors measured from manual and automatic activation maps.

	Manual map	Automatic map
Size of the 10 ms isochronal area		
AUC	0.72	0.48
Optimal threshold, cm^2	2.2	2.5
Sensitivity, %	83	33
Specificity, %	67	67
Accuracy, %	77	44
10 ms isochronal area longitudinal/perpendicular ratio		
AUC	0.84	0.94
Optimal threshold	0.91	1.27
Sensitivity, %	58	92
Specificity, %	100	100
Accuracy, %	72	94
Hypothesis-based threshold	1	1
Sensitivity,%	67	67
Specificity, %	83	100
Accuracy, %	72	78

AUC – area under the curve, SOO – site of origin.

ratio. A hypothesis-based threshold allows performing this comparison, showing slightly superiority of the automatic activation maps in the current patient sample (see Table 4).

The performance on SOO identification obtained in the present study was inferior to the perfect identification reported by Herczku *et al.* [4], which was achieved using only the 10 ms isochronal area longitudinal/perpendicular diameter ratio. On the other hand, using the diameter ratio in a study with a larger patient sample, Acosta *et al.* [9] reported results more similar to our hypothesis-based threshold (77% sensitivity and 100% specificity). In their work, SOO identification achieved 91% sensitivity and 100% specificity with the inclusion of a decision tree that incorporates the distance from the 10 ms EAS isochronal area to the pulmonary valve plane [9]. Therefore, the algorithm used for automatic activation mapping allows observer-independent measurements, and was superior to manual mapping for idiopathic VAs SOO identification in the current patient sample.

Limitations

The main study limitation was the lack of a balanced patient sample, especially for the RVOT SOO population. This produced sharp receiver operator curves, particularly in the specificity values (Fig. 4, bottom panels). This may explain the slight differences in optimal threshold values obtained in the current patient sample, compared to the literature [4,9]. Another possible source of error is the size of the mapping catheter tip (3.5 mm) used for mapping and ablation in this patient sample, which may sense far-field EGM from the other side of the septal separation between OTs. The use of catheters with smaller electrodes may also improve both signal quality and local electrical activation time measurements.

An additional limitation is the LAT definition used in this work. On one hand, the steepest downward slope of the unipolar EGM signal is known to be closely related with myocardial activation [15] but unipolar signals are prone to disruption by other electrical sources [5,15,16]; on the other hand, there is no clear consensus for LAT identification on bipolar EGMs [10,11]. However, the evaluated automatic mapping algorithm aims to provide a reliable LAT estimation based on the EGM signal onset that allows assessing activation pattern for automatic activation mapping in a robust and reproducible manner. Moreover, comparison with other proposed methods for automatic activation mapping is rather difficult. The proposal made by El Haddad *et al.* [17,18] does not compare automatic LAT identification with manual or audited annotations in a high number of mapping points. Finally, to our knowledge, there are no public reports about the LAT identification performance of the newly released CONFIDENSE module (Biosense Webster, Inc., Diamond Bar, CA, USA) for the CARTO system.

Conclusions

Automatic mapping of VAs based on the onset of the bipolar EGM signal allows fast, accurate and observer-independent assessment of LATs and activation propagation. Therefore, allowing precise identification of the EAS area and SOO and the characterization of the spreading of the idiopathic OTVAs activation sequence.

Acknowledgments

This study was supported by personal grants to A.A. refs.: BES-2011-046644 and EEBB-I-15-09466, by projects TEC2013-42140-R, DPI2016-75458-R and TIN2011-28067 from Ministerio de Economía y Competitividad. Also by Gobierno de Aragón (Spain) and European Social Fund (EU) through Grupo Consolidado BSICoS ref.: T 96. The CIBER-BBN is an initiative of Instituto de Salud Carlos III. This work was also supported in part by the project PI14/00759, integrated in the Plan Nacional de I + D + i and co-funded by the ISCIII-Subdirección General de Evaluación and the Fondo Europeo de Desarrollo Regional (FEDER).

Conflicts of interest

David Andreu is an employee of Boston Scientific Inc. The rest of authors declare that they have no conflict of interest.

Appendix A. Supplementary data

Supplementary data to this article can be found online at https://doi.org/10.1016/j.jelectrocard.2017.10.015.

References

[1] Aliot EM, Stevenson WG, Almendral-Garrote JM, Bogun F, Calkins CH, Delacretaz E, et al. EHRA/HRS expert consensus on catheter ablation of ventricular arrhythmias. Hear Rhythm 2009;6:886–933. https://doi.org/10.1016/j.hrthm.2009.04.030.
[2] Lerman BB, Stein KM, Markowitz SM. Mechanisms of idiopathic left ventricular tachycardia. J Cardiovasc Electrophysiol 1997;8:571–83. https://doi.org/10.1111/j.1540-8167.1997.tb00826.x.
[3] Movsowitz C, Schwartzman D, Callans DJ, Preminger M, Zado E, Gottlieb CD, et al. Idiopathic right ventricular outflow tract tachycardia: narrowing the anatomic location for successful ablation. Am Heart J 1996;131:930–6. https://doi.org/10.1016/S0002-8703(96)90175-1.
[4] Herczku C, Berruezo A, Andreu D, Armenta JF, Mont L, Borrà R, et al. Mapping data predictors of a left ventricular outflow tract origin of idiopathic ventricular tachycardia with V3 transition and septal earliest activation. Circ Arrhythmia Electrophysiol 2012;5:484–91. https://doi.org/10.1161/CIRCEP.111.969592.
[5] Issa ZF, Miller JM, Zipes DP. Clinical arrhythmology and electrophysiology: a Companion to Braunwald's heart disease. 2nd ed. Saunders; 2012.
[6] Prystowsky EN, Padanilam BJ, Joshi S, Fogel RI. Ventricular arrhythmias in the absence of structural heart disease. J Am Coll Cardiol 2012;59:1733–44. https://doi.org/10.1016/j.jacc.2012.01.036.
[7] Asirvatham SJ. Correlative anatomy for the invasive electrophysiologist: outflow tract and supravalvar arrhythmia. J Cardiovasc Electrophysiol 2009;20:955–68. https://doi.org/10.1111/j.1540-8167.2009.01472.x.
[8] Gami AS, Noheria A, Lachman N, Edwards WD, Friedman PA, Talreja D, et al. Anatomical correlates relevant to ablation above the semilunar valves for the cardiac electrophysiologist: a study of 603 hearts. J Interv Card Electrophysiol 2011;30:5–15. https://doi.org/10.1007/s10840-010-9523-3.
[9] Acosta J, Penela D, Herczku C, Macías Y, Andreu D, Fernández-Armenta J, et al. Impact of earliest activation site location in the septal right ventricular outflow tract for identification of left vs right outflow tract origin of idiopathic ventricular arrhythmias. Hear Rhythm 2015;12:726–34. https://doi.org/10.1016/j.hrthm.2014.12.029.
[10] Paul T, Moak JP, Morris C, Garson A. Epicardial mapping: how to measure local activation. Pacing Clin Electrophysiol 1990;13:285–92. https://doi.org/10.1111/j.1540-8159.1990.tb02042.x.
[11] Weiss C, Willems S, Rueppel R, Hoffmann M, Meinertz T. Electroanatomical mapping (CARTO) of ectopic atrial tachycardia: impact of bipolar and unipolar local electrogram annotation for localization the focal origin. J Interv Card Electrophysiol 2001;5:101–7. https://doi.org/10.1023/A:1009822328310.
[12] Alcaine A, Soto-Iglesias D, Calvo M, Guiu E, Andreu D, Fernández-Armenta J, et al. A wavelet-based electrogram onset delineator for automatic ventricular activation

mapping. IEEE Trans Biomed Eng 2014;61:2830–9. https://doi.org/10.1109/TBME.2014.2330847.
[13] Alcaine A, Soto-Iglesias D, Andreu D, Acosta J, Berruezo A, Laguna P, et al. A morphology-based spatial consistency algorithm to improve EGM delineation in ventricular electroanatomical mapping. Proc Comput Cardiol 2014;41:125–8 [Cambridge, MA (USA)].
[14] Lin L, Hedayat AS, Sinha B, Yang M. Statistical methods in assessing agreement: models, issues, and tools. J Am Stat Assoc 2002;97:257–70.
[15] Spach MS, Miller WT, Miller-Jones E, Warren RB, Barr RC. Extracellular potentials related to intracellular action potentials during impulse conduction in anisotropic canine cardiac muscle. Circ Res 1979;45:188–204.
[16] Eckardt L, Breithardt G. Construction and interpretation of endocardial maps: from basic electrophysiology to 3D mapping. In: Shenasa M, Hindricks G, Borggrefe M, Breithardt G, editors. Card. Mapp. 3rd ed. John Wiley & Sons, Inc.; 2009. p. 13–26.
[17] El Haddad M, Houben RPM, Stroobandt R, Van Heuverswyn F, Tavernier R, Duytschaever M. Algorithmic detection of the beginning and end of bipolar electrograms: implications for novel methods to assess local activation time during atrial tachycardia. Biomed Signal Process Control 2013;8:981–91.
[18] El Haddad M, Houben RPM, Stroobandt R, Van Heuverswyn F, Tavernier R, Duytschaever M. Novel algorithmic methods in mapping of atrial and ventricular tachycardia. Circ Arrhythm Electrophysiol 2014;7:463–72. https://doi.org/10.1161/CIRCEP.113.000833.